

Original Research Article

Open Access



In-depth characterization of a mouse model of postoperative atrial fibrillation

Joshua A. Keefe^{1,2} , Jose Alberto Navarro-Garcia^{1,2} , Li Ni³, Svetlana Reilly⁴ , Dobromir Dobrev^{2,5,6} ,
Xander H.T. Wehrens^{1,2,7,8,9,10} 

¹Cardiovascular Research Institute, Baylor College of Medicine, Houston, TX 77030, USA.

²Department of Integrative Physiology, Baylor College of Medicine, Houston, TX 77030, USA.

³Division of Cardiology, Department of Internal Medicine, Tongji Hospital, Tongji Medical College, Huazhong University of Science and Technology, Wuhan 430030, Hubei, China.

⁴Division of Cardiovascular Medicine, Radcliffe Department of Medicine, University of Oxford, John Radcliffe Hospital, Oxford OX3 9DU, UK.

⁵Institute of Pharmacology, University Duisburg-Essen, Essen 45122, Germany.

⁶Department of Medicine and Research Center, Montreal Heart Institute and Université de Montréal, Montréal, QC H1T 1C8, Canada.

⁷Department of Medicine, Baylor College of Medicine, Houston, TX 77030, USA.

⁸Department of Neuroscience, Baylor College of Medicine, Houston, TX 77030, USA.

⁹Department of Pediatrics, Baylor College of Medicine, Houston, TX 77030, USA.

¹⁰Center for Space Medicine, Baylor College of Medicine, Houston, TX 77030, USA.

Correspondence to: Dr. Xander H.T. Wehrens, Cardiovascular Research Institute, Baylor College of Medicine, One Baylor Plaza, BCM335, Houston, TX 77030, USA. E-mail: wehrens@bcm.edu

How to cite this article: Keefe JA, Navarro-Garcia JA, Ni L, Reilly S, Dobrev D, Wehrens XHT. In-depth characterization of a mouse model of postoperative atrial fibrillation. *J Cardiovasc Aging* 2022;2:40. <https://dx.doi.org/10.20517/jca.2022.21>

Received: 14 Jun 2022 **First Decision:** 5 Jul 2022 **Revised:** 14 Jul 2022 **Accepted:** 14 Jul 2022 **Published:** 19 Jul 2022

Academic Editor: Ali J. Marian **Copy Editor:** Fangling Lan **Production Editor:** Fangling Lan

Abstract

Introduction: Postoperative atrial fibrillation (POAF), characterized as AF that arises 1-3 days after surgery, occurs after 30%-40% of cardiac and 10%-20% of non-cardiac surgeries, and is thought to arise due to transient surgery-induced triggers acting on a preexisting vulnerable atrial substrate often associated with inflammation and autonomic nervous system dysfunction. Current experimental studies often rely on human atrial tissue samples, collected during surgery prior to arrhythmia development, or animal models such as sterile pericarditis and atriotomy, which have not been robustly characterized.



© The Author(s) 2022. **Open Access** This article is licensed under a Creative Commons Attribution 4.0 International License (<https://creativecommons.org/licenses/by/4.0/>), which permits unrestricted use, sharing, adaptation, distribution and reproduction in any medium or format, for any purpose, even commercially, as long as you give appropriate credit to the original author(s) and the source, provide a link to the Creative Commons license, and indicate if changes were made.



Aim: To characterize the demographic, electrophysiologic, and inflammatory properties of a POAF mouse model.

Methods and Results: A total of 131 wild-type C57BL/6J mice were included in this study. A total of 86 (65.6%) mice underwent cardiothoracic surgery (THOR), which consisted of bi-atrial pericardiectomy with 20 s of aortic cross-clamping; 45 (34.3%) mice underwent a sham procedure consisting of dissection down to but not into the thoracic cavity. Intracardiac pacing, performed 72 h after surgery, was used to assess AF inducibility. THOR mice showed greater AF inducibility (38.4%) compared to Sham mice (17.8%, $P = 0.027$). Stratifying the cohort by tertiles of age showed that the greatest risk of POAF after THOR compared to Sham occurred in the 12-19-week age group. Stratifying by sex showed that cardiothoracic (CT) surgery increased POAF risk in females but had no significant effect in males. Quantitative polymerase chain reaction of atrial samples revealed upregulation of transforming growth factor beta 1 (*TGF- β 1*) and interleukin 6 (IL6) and 18 (IL18) expression in THOR compared to Sham mice.

Conclusion: Here, we demonstrate that the increased POAF risk associated with CT surgery is most pronounced in female and 12-19-week-old mice, and that the expression of inflammatory cytokines is upregulated in the atria of THOR mice prone to inducible AF.

One sentence summary: We developed a mouse model of POAF that replicates key features of this condition in humans in terms of incidence and inflammatory indices. We demonstrated that female mice have a greater POAF risk than males, highlighting the importance of considering biological sex in future POAF mouse studies.

Keywords: Atrial fibrillation, cardiothoracic surgery, biological sex, inflammation, fibrosis

INTRODUCTION

Atrial fibrillation (AF) is the most common arrhythmia and affects 4% of adults older than 60^[1]. Common risk factors for AF include hypertension, valvular heart disease, heart failure, obstructive sleep apnea, obesity, and chronic kidney disease^[2]. One important risk factor for AF is surgery, and AF developing during the days following surgery is termed postoperative AF (POAF). POAF typically occurs 1-3 days after surgery^[3] and portends a 5-fold higher risk of chronic AF^[4] and a 2-fold higher risk of stroke and mortality^[5,6]. Rates of POAF are 15%-42% after cardiac surgery^[7] and 10%-20% after non-cardiac surgery^[6,8,9].

POAF is thought to arise due to transient triggers such as autonomic activation and post-surgical inflammation acting on a preexisting substrate to promote triggered activity and reentry^[9]. Evidence for the role of autonomic activation comes from the significant reduction in POAF with beta-blocker therapy^[10] as well as higher circulating norepinephrine^[11] and aldosterone^[12] levels observed in POAF patients. Evidence for the role of inflammation is less consistent among experimental studies, but higher preoperative and postoperative white blood cell counts are seen in POAF patients^[13]. Structural and cellular alterations such as left atrial fibrosis^[14] and decreased atrial autophagy^[15] have also been linked to POAF development in mice.

Experimental studies of POAF are limited. Human atrial tissue samples provide information about predisposing substrate but are typically collected during the surgical procedure days prior to POAF development and thus do not provide information about the substrate at the time of arrhythmia initiation. Current animal models of POAF include sterile pericarditis, pericardiectomy, and atriotomy^[16-18]. However, unlike in the clinical setting with patients undergoing cardiac surgery, the currently available mouse models do not account for the ischemic and hemodynamic insults inherent to cardiac surgery. Moreover, to our knowledge, a comprehensive and powered analysis of the electrophysiologic (EP) and AF inducibility of these models in a large cohort of mice has not been conducted. Here, we describe a model of POAF

consisting of a bi-atrial pericardiectomy with cross-clamping of the thoracic aorta to simulate cardiothoracic (CT) surgery. We systematically characterize the AF inducibility and inflammatory EP signature in our POAF model using over 100 wild-type mice.

MATERIALS AND METHODS

Mouse colonies: All experiments were carried out using wild-type male and female C57BL/6J mice purchased from Jackson Labs (strain #000664).

Experimental protocols: Experiments were carried out according to NIH Guidelines on the Use of Laboratory Animals. All procedures were approved by the Baylor College of Medicine Institutional Animal Care and Use Committee, protocol number AN-4044. A total of 131 mice (48% male) were included in this study (45 Sham, 86 THOR). All animals were given one injection of buprenorphine subcutaneously at a dose of 1 mg/kg at least 1 h before surgery. Animals were monitored every day after surgery until terminal EP studies were performed 72 h after the surgery. Meloxicam, which is often administered every 24-48 h postoperatively in mice, was withheld per protocol due to the potential confounding effect of its non-steroidal anti-inflammatory mechanism of action on the pathways involved in POAF (see Discussion).

Animal model: Our mouse model of POAF was designed to recapitulate CT surgery [Figure 1]. Anesthesia was induced by placing mice in an induction chamber filled with 4% isoflurane in 100% oxygen until the mice lost consciousness. Mice were intubated and ventilated at a tidal volume of 150 μ L and respiratory rate of 175 breaths/minute, and anesthesia was maintained using 2.5% v/v isoflurane in 100% oxygen. Body temperature was maintained at $37.0\text{ }^{\circ}\text{C} \pm 0.5\text{ }^{\circ}\text{C}$ using a heated platform guided by a rectal thermometer. After dissection through the skin and subcutaneous tissue, the pectoralis major and minor muscles were separated laterally and the thoracic cavity was exposed through the 2nd or 3rd intercostal space [Figure 1A]. Bi-atrial pericardiectomy [Figure 1B and C] and cross-clamping of the thoracic aorta for 20 s [Figure 1D] were performed. For the sham procedure, the same skin and muscle dissection was performed, but the chest cavity was not entered.

Programmed electrical stimulation: 72 h after CT surgery, AF inducibility was analyzed by performing a right heart catheterization to conduct intracardiac pacing as previously described^[19]. Briefly, the mouse was anesthetized (1.75% v/v isoflurane in 100% oxygen). The subcutaneous tissue superficial to the right external jugular vein was dissected, and proximal and distal control of the right external jugular vein was secured with 6-0 sutures. A 1.1F octapolar catheter (EPR-800, Millar Instruments, Houston, TX) was then inserted into the right external jugular vein, through the superior vena cava, and into the right atrium and ventricle. Correct placement of the catheter was verified by looking for the appropriate P wave deflection after intra-atrial pacing and the appropriate QRS deflection after intra-ventricular pacing. All EP protocols were performed at 1.75% v/v, isoflurane/oxygen and rectal temperature between $37.0\text{ }^{\circ}\text{C} \pm 0.5\text{ }^{\circ}\text{C}$.

Following baseline recordings, the sinus node recovery time (SNRT) was determined by pacing the right atrium at a basic cycle length (BCL) of 100 milliseconds (ms) for 15 s and then measuring the amount of time from the last pacing impulse until the first spontaneous sinoatrial node beat^[20]. The SNRT was repeated at a BCL of 90 ms. The atrial effective refractory period (AERP) was determined by applying a series of atrial pacing trains at a BCL of 100 ms, each with a coupled premature stimulus at the end (referred to as S2). The S1-S2 was decreased by 2 ms from 70 ms to 20 ms. The AERP was defined as the longest S1-S2 interval that failed to propagate into the ventricles. AF inducibility was determined by performing the A-burst protocol^[21], which applies a series of 2-s bursts starting at a BCL of 40 ms. Each 2-s burst decreases the BCL by 2 ms until a BCL of 20 ms is reached. The burst pacing protocol was performed in triplicate per mouse

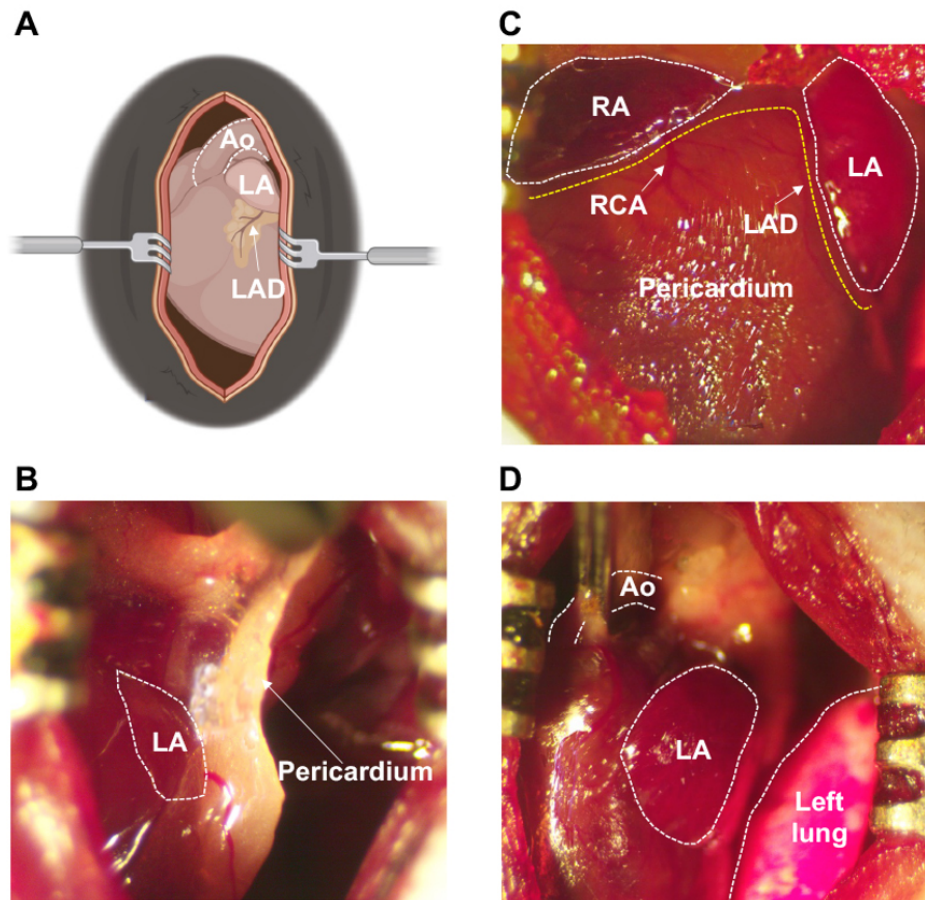


Figure 1. Cardiothoracic surgery workflow. (A) Schematic illustration of exposed chest cavity following dissection through 2nd or 3rd intercostal space. (B) Fibrous pericardium covering the left atrium prior to pericardiectomy. (C) Status after bi-atrial pericardiectomy for both atria, with pericardium removed. (D) Cross-clamping of ascending aorta. Ao: Aorta; LA: left atrium; LAD: left anterior descending coronary artery; RA: right atrium; RCA: right coronary artery.

and AF inducibility was defined as a positive AF event lasting at least one second in at least two (out of three) positive events. A positive AF event was defined by irregularly irregular RR intervals without discernable P waves on electrocardiogram (ECG).

RNA isolation and cDNA preparation: Total RNA was isolated from the atrial appendages of six Sham mice without AF and six THOR mice with AF. Tissue was harvested immediately after EP pacing. Both the left and right atrial appendages were used for all samples. After harvesting, the heart underwent retrograde perfusion with cold phosphate-buffered saline. Atrial samples were then frozen in liquid nitrogen for 5 min and stored at -80°C . To isolate total RNA, atrial samples were ground up and then $200\ \mu\text{L}$ of TRIzol (Ambion) was added to each sample. Samples were spun down the samples for 60 s at 16,000 rpm. The Direct-zol RNA MiniPrep (Zymo Research) was used to isolate total RNA. RNA concentrations were measured using a nanodrop and stored at -80°C . To generate cDNA, reverse transcription was carried out using the iScript Reverse Transcription Supermix (BioRad) with 500 ng of RNA per sample.

qPCR: Quantitative polymerase chain reaction (qPCR) was conducted for *IL-6*, *IL-1*, *IL-18*, *IL-10*, interferon gamma (*IFN- γ*), tumor necrosis factor alpha (*TNF- α*), and *TGF- β 1* with the primers listed in [Supplementary Table 1](#). Three technical replicates were performed per sample. Six individual biological

replicates were used per group (six Sham and six THOR mice). A total of 10 μL reaction solution was used per well: 5 μL of SYBR Green Master Mix (Thermo Fisher Scientific), 0.5 μL of 40 \times Yellow Sample Buffer (Thermo Fisher Scientific), 1 μL of 10 μM forward primer, 1 μL of 10 μM reverse primer, 2 μL of cDNA (prepped as described above), and 3 μL of distilled water. Fold changes in gene expression were calculated using the delta-delta Ct method as previously described^[22]. Gene expression fold changes (relative to *GAPDH*) in THOR mice were then normalized to those in Sham mice by dividing by the average Sham fold change. To compare gene expression between Sham and THOR mice, two-sample *t*-tests were conducted comparing the delta-delta Ct values due to the non-linearity of the fold-change values.

Statistical analyses: All statistical analyses were performed using RStudio version 1.4.1717 and GraphPad Prism version 9.3.1. Two-sided *P* values less than 0.05 were considered statistically significant. Chi-square tests were performed for categorical independent and dependent variable data. Fisher's exact tests were used in lieu of chi-square tests when expected counts were less than five in any group. Two-sample *t*-tests were performed for binary independent and continuous dependent variable data. Wilcoxon rank-sum tests were used in lieu of 2-sample *t*-tests when the dependent variable was ordinal (e.g., number of AF events). Outliers were defined as > 2 standard deviations above or below the mean.

RESULTS

Baseline characteristics: A total of 131 mice (48% male) were included in the study - 45 Sham and 86 THOR. Intraoperative mortality was 4% ($N = 5$ deaths) due to bleeding complications. Mice who died intraoperatively were not included in final mouse counts or subsequent analyses. Mice ages ranged from 7- to 27-week-old (median age was 14 weeks). Mice were analyzed by sex and tertiles of age (≤ 11 weeks, 12-19 weeks, and ≥ 20 weeks). ECG metrics are shown by treatment group [Table 1], tertiles of age [Table 2], sex [Table 3], and AF inducibility [Table 4]. All pairwise comparisons between groups did not reach statistical significance except for the comparison of PR interval by age group (ANOVA $P = 5.6\text{E-}05$). Subsequent pairwise comparisons demonstrated that PR interval differed between the ≤ 11 -week vs. ≥ 20 -week ($P = 5.2\text{E-}05$) and the 12-19-week vs. ≥ 20 -week ($P = 0.016$) age groups but not the ≤ 11 -week vs. 12-19-week age group ($P = 0.023$) at Bonferroni significance ($P < 0.017$, results not shown).

Overall AF inducibility: In the overall study, 33 out of 86 (38.4%) THOR mice exhibited inducible POAF, while 8 out of 45 (17.8%) Sham mice had POAF. Representative ECG tracings showing sinus rhythm and AF are shown in Figure 2A. The proportion of POAF events in THOR mice was greater than IN Sham mice ($P = 0.027$, Figure 2B). The number of inducible AF events (out of three) was higher in THOR vs. Sham mice ($P = 0.0089$, Figure 2C). These results were primarily driven by the greater number of THOR mice with 2 (out of 3) AF events [Figure 2C], since the proportion of THOR and Sham mice with 3 (out of 3) was similar. Of the mice who had POAF, the AF duration trended longer in THOR mice (mean = 34.9 s) compared to Sham (mean = 30.2 s), but the difference was not statistically significant ($P = 0.41$, Figure 2D).

AF inducibility by age: Mice were analyzed according to tertiles of age to identify an age range at which the difference in AF inducibility after cardiac surgery differed the most between sham and THOR mice. Odds of inducible POAF in THOR were similar to Sham in the youngest tertile (odds ratio [OR] = 0.97) and greater than Sham in the middle (OR = 11.7) and older (OR = 3.11) tertiles [Figure 3A-C]. Only the middle tertile (12-19 weeks old) showed a statistically significant difference in AF inducibility ($P = 8.2\text{E-}03$, Figure 3B). The number of AF events was nominally significantly different between Sham and THOR mice in the youngest ($P = 0.075$) and middle ($P = 0.053$) tertiles [Supplementary Figure 1].

Table 1. Baseline ECG and EP characteristics by treatment group

	Sham (mean ± SEM)	THOR (mean ± SEM)	P value
N (%)	45 (34.3%)	86 (65.5%)	NA
RR (ms)	117 ± 2.4	113 ± 1.4	0.078
P wave duration (ms)	12.0 ± 0.026	12.1 ± 0.015	0.56
PR (ms)	42.9 ± 0.57	41.8 ± 0.39	0.11
QRS (ms)	16.9 ± 0.37	17.2 ± 0.34	0.67
SNRT100 (ms)	139 ± 5.8	145 ± 5.1	0.47
AERP100 (ms)	48.6 ± 1.2	46.9 ± 1.0	0.25

ECG: Electrocardiogram; AERP: atrial effective refractory period; ms: milliseconds; SNRT: sinus node recovery time.

Table 2. Baseline ECG and EP characteristics by age

	≤ 11 weeks (mean ± SEM)	12-19 weeks (mean ± SEM)	≥ 20 weeks (mean ± SEM)	P value
N (%)	47 (35.9%)	47 (35.9%)	37 (28.2%)	NA
Female (%)	18 (38.3%)	29 (60.4%)	21 (56.8%)	NA
RR (ms)	112 ± 2.0	114 ± 1.8	118 ± 2.8	0.20
P wave duration (ms)	12.3 ± 0.027	12.0 ± 0.026	11.9 ± 0.034	0.47
PR (ms)	40.6 ± 0.49	42.2 ± 0.45	44.1 ± 0.64	5.6E-05
QRS (ms)	16.3 ± 0.39	17.3 ± 0.55	17.7 ± 0.30	0.091
SNRT100 (ms)	148 ± 6.6	150 ± 7.4	128 ± 5.0	0.059
AERP100 (ms)	48.2 ± 1.0	48.0 ± 1.3	46.0 ± 1.8	0.49

ECG: Electrocardiogram; AERP: atrial effective refractory period; ms: milliseconds; SNRT: sinus node recovery time.

Table 3. Baseline ECG and EP characteristics by sex

	Female (mean ± SEM)	Male (mean ± SEM)	P value
N (%)	68	63	NA
RR (ms)	115 ± 1.8	113 ± 1.7	0.45
P wave duration (ms)	12.0 ± 0.018	12.2 ± 0.021	0.36
PR (ms)	42.2 ± 0.44	42.1 ± 0.50	0.93
QRS (ms)	16.9 ± 0.30	17.3 ± 0.44	0.46
SNRT100 (ms)	145 ± 5.5	141 ± 5.6	0.63
AERP100 (ms)	47.9 ± 1.1	47.1 ± 1.1	0.64

ECG: Electrocardiogram; AERP: atrial effective refractory period; ms: milliseconds; SNRT: sinus node recovery time.

Table 4. Baseline ECG and EP characteristics by AF inducibility

	AF negative (mean ± SEM)	AF positive (mean ± SEM)	P value
N (%)	90 (68.7%)	41 (31.3%)	NA
Female (N [%])	46 (51%)	22 (53.6%)	NA
RR (ms)	114 ± 1.5	115 ± 2.2	0.80
P wave duration (ms)	12.0 ± 0.015	12.3 ± 0.026	0.22
PR (ms)	42.0 ± 0.40	42.4 ± 0.55	0.58
QRS (ms)	17.1 ± 0.35	17.0 ± 0.35	0.83
SNRT100 (ms)	140 ± 4.4	151 ± 7.9	0.27
AERP100 (ms)	47.4 ± 0.98	47.8 ± 1.3	0.81

ECG: Electrocardiogram; AF: atrial fibrillation; AERP: atrial effective refractory period; ms: milliseconds; SNRT: sinus node recovery time.

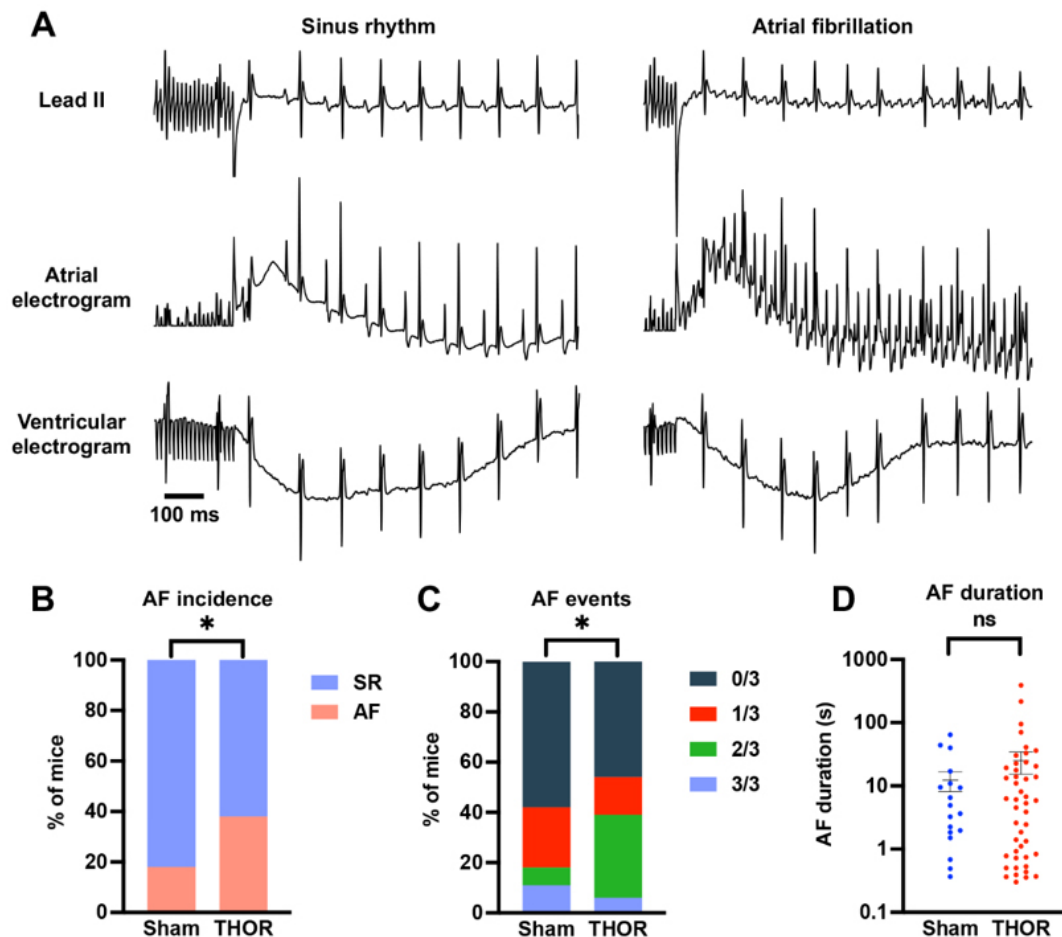


Figure 2. (A) Representative ECG tracings showing sinus rhythm (left) and AF (right) after the intracardiac burst atrial burst protocol. (B) Percent of mice in sinus rhythm (blue) and AF (red) in Sham ($n = 45$) and THOR ($n = 86$) mice. AF was defined as at least two (out of three) positive AF events after the A-burst protocol. (C) Percent of mice with zero, one, two, and three events after the A-burst protocol in Sham ($n = 45$) and THOR ($n = 86$) mice. (D) AF duration in Sham ($n = 19$) and THOR ($n = 46$) mice. Only mice with inducible AF episodes are included. Values plotted are equal to the sum of AF duration over the three A-burst protocols. Data are reported as mean \pm SEM. P values in panels (B and C) were obtained from chi-square tests. P value in panel (D) was obtained from two-sample Student's t -tests. $*P < 0.05$. $P \geq 0.05$ denoted ns. ECG: Electrocardiogram; AF: atrial fibrillation; SR: sinus rhythm.

AF inducibility by sex: The odds of POAF were greater in male and female THOR mice. Only female mice exhibited statistically significantly greater AF inducibility after THOR compared to Sham ($P = 6.9E-03$, Figure 4A). There was no significant difference in AF inducibility between THOR and Sham male mice ($P = 0.71$, Figure 4B). Female THOR mice had a statistically significantly greater number of AF events compared to Sham ($P = 0.039$, Supplementary Figure 2A). There was no difference in the number of AF events for male Sham vs. THOR mice ($P = 0.15$, Supplementary Figure 2B).

PCR amplification of inflammatory genes: Gene expression of *IL-6*, *IL-1 β* , *IL-18*, *IL-10*, *IFN- γ* , *TNF- α* , and *TGF- β 1* was evaluated by qPCR in atrial tissue of six Sham and six THOR mice. GAPDH was used as the housekeeping gene. Normalized fold changes of gene expression (relative to the Sham group) are shown in Figure 5. Compared to Sham, THOR mice had a statistically significantly greater expression of *IL-6* ($P = 1.82E-04$, Figure 5A), *IL-18* ($P = 1.7E-03$, Figure 5B), and *TGF- β 1* ($P = 0.046$, Figure 5C). There were no statistically significant differences in *IL-1 β* , *IL-10*, *IFN- γ* , and *TNF- α* expression between Sham and THOR mice [Supplementary Figure 3].

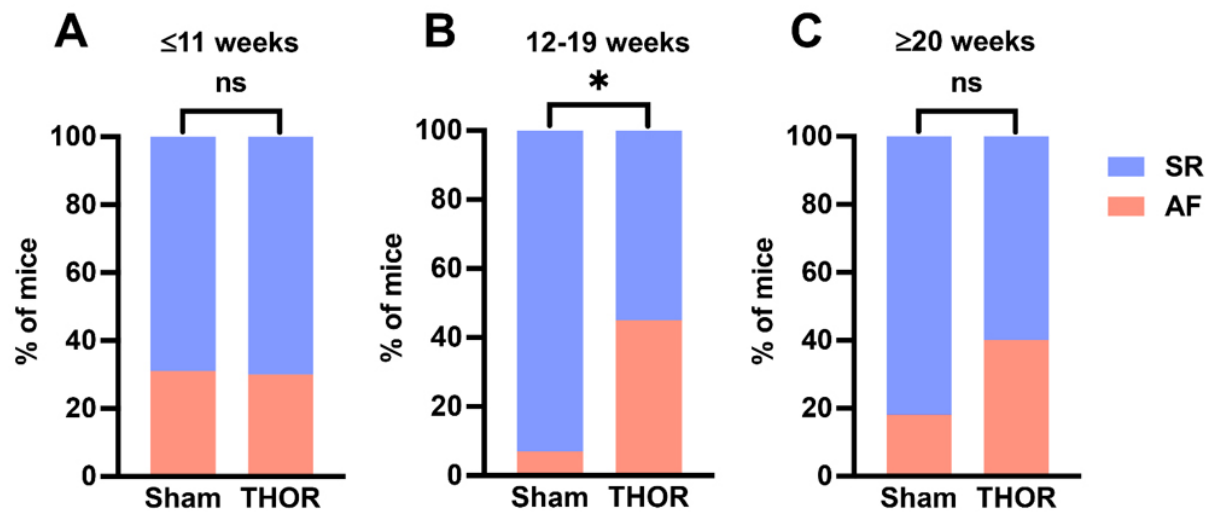


Figure 3. AF inducibility by age. (A) Percent of mice in sinus rhythm (blue) and AF (red) in Sham ($n = 14$) and THOR ($n = 33$) mice in the bottom age tertile. (B) Percent of mice in sinus rhythm (blue) and AF (red) in Sham ($n = 14$) and THOR ($n = 34$) mice in the middle age tertile. (C) Percent of mice in sinus rhythm (blue) and AF (red) in Sham ($n = 17$) and THOR ($n = 20$) mice in the oldest age tertile. AF was defined as at least two (out of three) positive AF events after the A-burst protocol. P values were obtained from chi-square tests. $*P < 0.05$. $P \geq 0.05$ denoted ns. AF: Atrial fibrillation; SR: sinus rhythm.

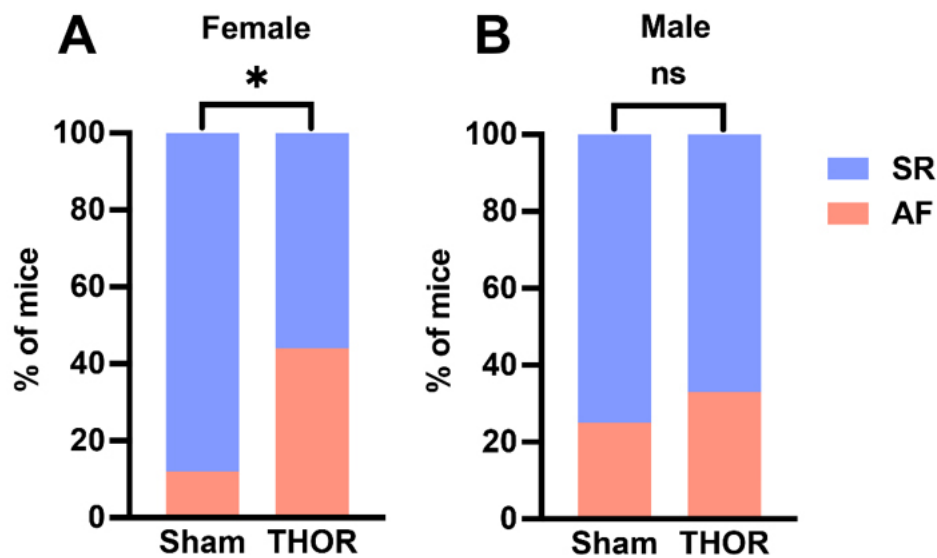


Figure 4. AF inducibility by sex. (A) Percent of female mice in sinus rhythm (blue) and AF (red) in $n = 16$ Sham and $n = 52$ THOR mice. (B) Percent of male mice in sinus rhythm (blue) and AF (red) in $n = 10$ Sham and $n = 53$ THOR mice. AF was defined as at least two (out of three) positive AF events after the A-burst protocol. P values were obtained from chi-square tests. $*P < 0.05$. $P \geq 0.05$ denoted ns. AF: Atrial fibrillation; SR: sinus rhythm.

DISCUSSION

In this study, we characterized a novel mouse model of POAF in a cohort of 131 mice. The surgery-related mortality in our study was around five percent. All mortalities occurred intraoperatively due to bleeding complications at an incidence of ~4%, which is similar to that associated with coronary artery bypass grafting in humans (3%)^[23]. No mice died during the 72 h postoperative period. The absolute risk of developing POAF during the first three days post-surgery was 38.4% (33/86) in THOR and 17.8% (8/45) in

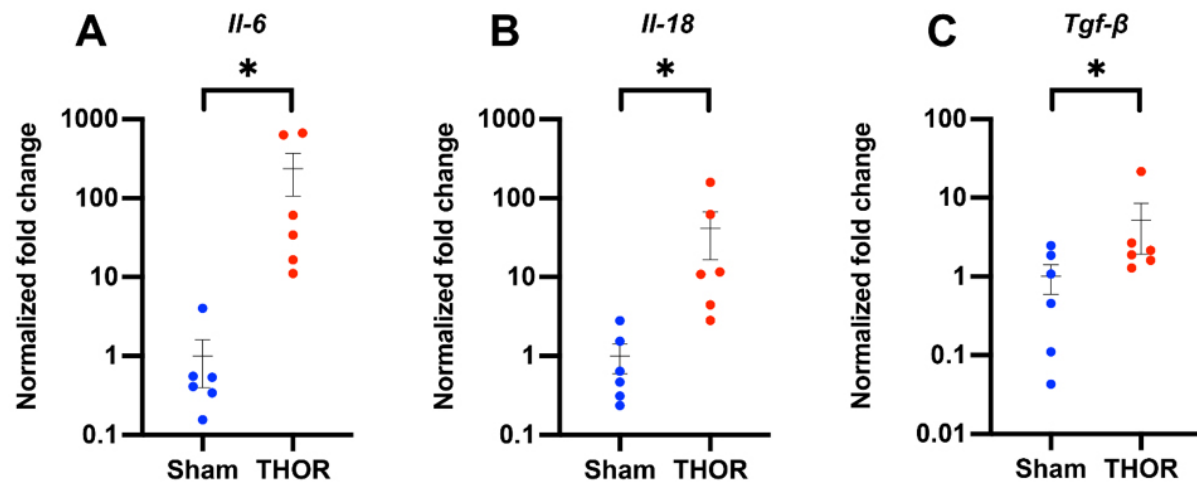


Figure 5. qPCR amplification of *IL-6*, *IL-18*, and *TGF-β1* mRNA levels in atrial tissue. Normalized fold changes of gene expression (relative to *Gapdh*) in *IL-6* (A), *IL-18* (B), and *TGF-β1* (C) calculated using the delta-delta CT method. * $P < 0.05$. $P \geq 0.05$ denoted ns. $n = 6$ Sham, $n = 6$ THOR mice. qPCR: Quantitative polymerase chain reaction.

Sham mice, corresponding to a 2.87-fold increase in odds of POAF in THOR compared to Sham mice. This effect size is comparable to POAF in humans, which occurs in ~30% of patients after cardiac surgery^[24], although our study assessed the incidence of inducible but not spontaneous AF. The inducibility of AF is an index for the development of an AF-maintaining substrate and is commonly assessed in non-surgical mouse models since only a few (transgenic) mouse lines exhibit spontaneous AF^[25,26]. As AF in mice requires supraphysiologic triggers, baseline POAF risk may be higher than those seen in humans, but this increase in risk may be negated by the healthy baseline status of mice in our study compared to humans undergoing cardiac surgery.

Impact of age on POAF risk

We sought to explore putative differences in risk of POAF by age and sex. We first analyzed POAF incidence by tertiles of age. The risk of POAF was greatest in the middle (12-19-week) tertile (odds ratio [OR] = 11.7, $P = 8.2E-03$). While the overall incidence of POAF was greater in the oldest tertile, the difference in POAF incidence between Sham and THOR mice was smaller due to the higher POAF incidence in Sham mice. Older age is a well-established risk factor for AF in humans^[27], and POAF clinical risk score algorithms include age > 60 years old, which portends a 2-4-fold increase in POAF risk^[28]. In mice, Jansen *et al.* showed that the incidence of inducible AF in mice positively correlates with age - from 20% in 20-week-old to 40% in 60-week-old WT mice^[29]. Loss of natriuretic peptide signaling was implicated as a key driver of the increase in AF susceptibility in older mice due to increased atrial fibrosis and shortened action potential duration. Other studies have demonstrated similar increases in AF susceptibility and atrial fibrosis^[30], as well as attenuated heart rate variability (i.e., altered sympathetic/parasympathetic balance)^[31] with aging in mice.

Impact of sex on POAF risk

In humans, the male sex is associated with a 3-fold greater risk of POAF after cardiac surgery^[32]. However, biological sex was not included in the risk score published by Mariscalco *et al.* due to its poor prognostic value for arrhythmia development in the regression model^[28]. Nonetheless, our study demonstrated that female mice had significantly greater odds of POAF (OR = 5.82) compared to males (OR = 1.45); this is seemingly the opposite of what one would expect from human observations. In humans, AF affects males (77.5 per 1000 person-years) more than females (59.5 per 1000 person-years)^[33]. However, AF in females is

associated with more severe clinical sequelae such as embolic stroke^[34] and mortality^[33]. One explanation for this difference in clinical outcome is that females with AF are more likely affected by valvular heart disease while males with AF tend to be affected by coronary artery disease^[35]. Valvular AF is well-known to portend a significantly greater risk of stroke (17-fold increase) compared to nonvalvular AF (5-fold increase)^[36]. Since we used relatively young mice with no known propensity to valvular heart disease or coronary artery disease, the absence of these comorbidities may have shifted the sex-specific risk for POAF.

In our study, we assessed the risk of inducible AF, which determines the presence of an arrhythmia-permissive substrate rather than the occurrence of spontaneous triggers of arrhythmias. In humans, one might hypothesize that females have a more AF-prone substrate compared to males but perhaps lack the AF triggers. Indeed, the lower success of AF catheter ablation in females is thought to occur partly due to the greater atrial fibrosis seen in females with long-standing AF compared to females without AF. The same increase in fibrosis does not occur in males with long-standing AF^[37].

In our mouse model, *TGF-β*, a key pro-fibrotic regulator, was upregulated in THOR mice with POAF compared to Sham. While fibrosis may be thought of as a more indolent process not directly involved in POAF, our results may reflect the initial activation of myofibroblasts in response to the damage due to CT surgery. Indeed, prior studies have demonstrated that myofibroblasts are activated in mice within three days of cardiac insults such as ischemia^[38] and stretch^[39]. To further explore the effects of sex, we conducted qPCR comparing POAF-free female vs. male mice [Supplementary Figure 4]. Results suggest that female sham mice have greater *TGF-β* expression than male sham mice ($P = 0.039$), perhaps suggesting greater baseline fibrosis in female mice. Taken together, our results showing greater POAF incidence in female mice may reflect a sex difference in the propensity toward atrial fibrotic remodeling following CT surgery.

Role of inflammation in postoperative AF

Postoperative inflammation is an important risk factor associated with POAF^[40]. To this end, we withheld meloxicam, which is usually given every 24-48 h postop, in our CT surgery model. We then sought to explore whether our model induces a local atrial inflammatory response; thus, we conducted a qPCR analysis to measure the expression of proinflammatory cytokines in atrial tissue. Results demonstrated statistically significant upregulations of *IL-6*, *IL-18*, and *TGF-β1* in THOR compared to Sham mice. We did not find increases in proinflammatory cytokines *IL-1β* and *TNF-α* in THOR mice. While partially attributable to the relatively large biological variance among samples, these results could also indicate that regulation of these cytokines occurs post-translationally and/or that systemic (rather than local) cytokine levels are more likely affected. Indeed, a recent study demonstrated lower *IL-1β* protein expression in atrial cardiomyocytes from POAF patients^[41] due to the pore-forming effects of gasdermin D, which increased systemic *IL-1β* levels. Nonetheless, prior studies have reported increases in inflammatory mediators such as *TNF-α*^[42], *IL-6*^[43], *IL-1β*^[44], and *NLRP3*^[45] activation in POAF. Exposure of human atrial cardiomyocytes to *IL-1β* has been shown to reproduce the POAF-associated cellular proarrhythmic phenotype characterized by delayed afterdepolarizations^[45]. Altogether, we show evidence that our CT surgery model induces a local inflammatory response in the atria.

Study limitations

Our study has several limitations. First, we quantified gene expression, which may not reflect protein expression and/or serum levels. Second, the relatively large within-group variance among biological replicates used in our qPCR experiments may have precluded the determination of additional statistically significant differences in gene expression. Third, we did not differentiate between left and right atrium. The expression of ion channels, inflammatory and fibrotic mediators, and thrombogenic proteins differs between atria in humans^[46] and mice^[47]. Fourth, our study focuses on inducible, not spontaneous, AF, which

is a surrogate parameter of the AF-maintaining substrate rather than a trigger. In addition, EP studies were conducted in anesthetized mice (at 1.75% v/v isoflurane/oxygen). While prior studies suggest that cardiovascular depression does not occur at an isoflurane dose of 1.75%^[48,49], it is possible that sub-physiologic alterations in cardiac conduction could have altered AF susceptibility. Fifth, the Sham mice in the youngest tertile had a relatively high incidence (44%) of AF. This was partly due to the male predominance (62%) in this age group, as three (out of the four) Sham mice with AF were male. Female Sham mice in this age group had an AF incidence of 16.7%, which is slightly lower than the overall AF incidence in Sham mice (17.8%). Finally, the mice used in our study had healthy atria at baseline, which precluded the assessment of the role of the preexisting atrial substrate which is created by risk factors and comorbidities in patients. Moreover, the mice in this study were relatively young (range 7-27 weeks) as the mean age of the oldest mouse tertile corresponded to a human age of ~31 years. Taken together, the healthy baseline state and relatively young mouse ages used in this study limit the clinical translatability of our results and may partially account for the different sex-specific POAF risk profiles in our mice compared to humans.

In conclusion, we characterized a mouse model of POAF induced by a CT surgical procedure. We show that the risk of POAF is most pronounced in females and 12-19-week-old mice. We also show that key fibrosis (*TGF-β1*) and inflammatory (*IL-6*, *IL-18*) genes are upregulated postoperatively in our model. Taken together, our POAF model recapitulates key aspects of human AF, and we provide evidence that future POAF mouse studies should consider the effects of sex and age.

DECLARATIONS

Acknowledgments

The authors are grateful to Elda M. Munivez.

Authors' contributions

Made substantial contributions to conception, study design, and data interpretation: Keefe JA, Navarro-Garcia JA, Ni L, Dobrev D, Wehrens XHT

Conducted experiments and data analysis: Keefe JA, Navarro-Garcia JA, Ni L

Drafted the manuscript: Keefe JA

Funding: Ni L, Reilly S, Dobrev D, Wehrens XHT

Availability of data and materials

All data will be available upon request to Wehrens XHT.

Financial support and sponsorship

This work was supported by National Institutes of Health grants R01-HL131517, R01-HL136389, R01-HL089598, and R01-HL163277 (to Dobromir Dobrev) and R01-HL147108, R01-HL153350, and R01-HL089598 (to Xander H.T. Wehrens), the German Research Foundation (DFG) grant Do 769/4-1 (to Dobromir Dobrev), and the European Union (large-scale integrative project MAESTRIA, No. 965286 to Dobromir Dobrev), the British Heart Foundation Intermediate Fellowship FS/SBSRF/2231026 (to Svetlana Reilly), the National Natural Science Foundation of China No. 82070354 (to Li Ni), and Program for Huazhong University of Science and Technology Academic Frontier Youth Team (No. 2019QYTD08) (to Li Ni). The Robert and Janice MacNair Foundation McNair MD/PhD Scholars Program (Joshua A. Keefe), and the Baylor College of Medicine Medical Scientist Training Program (Joshua A. Keefe).

Conflicts of interest

All authors declared that there are no conflicts of interest.

Ethical approval and consent to participate

All mouse surgeries were approved by the Baylor College of Medicine's Institutional Animal Care and Use Committee, protocol number AN-4044.

Consent for publication

Not applicable.

Copyright

© The Author(s) 2022.

REFERENCES

1. Go AS, Hylek EM, Phillips KA, et al. Prevalence of diagnosed atrial fibrillation in adults: national implications for rhythm management and stroke prevention: the anticoagulation and risk factors in atrial fibrillation (ATRIA) study. *JAMA* 2001;285:2370-5. [DOI](#) [PubMed](#)
2. Shamloo AS, Dagues N, Arya A, Hindricks G. Atrial fibrillation: a review of modifiable risk factors and preventive strategies. *Rom J Intern Med* 2019;57:99-109. [DOI](#) [PubMed](#)
3. Echahidi N, Pibarot P, O'Hara G, Mathieu P. Mechanisms, prevention, and treatment of atrial fibrillation after cardiac surgery. *J Am Coll Cardiol* 2008;51:793-801. [DOI](#) [PubMed](#)
4. Lee SH, Kang DR, Uhm JS, et al. New-onset atrial fibrillation predicts long-term newly developed atrial fibrillation after coronary artery bypass graft. *Am Heart J* 2014;167:593-600.e1. [DOI](#) [PubMed](#)
5. Lin MH, Kamel H, Singer DE, Wu YL, Lee M, Ovbiagele B. Perioperative/postoperative atrial fibrillation and risk of subsequent stroke and/or mortality. *Stroke* 2019;50:1364-71. [DOI](#)
6. Caldonazo T, Kirov H, Rahouma M, et al. Atrial fibrillation after cardiac surgery: a systematic review and meta-analysis. *J Thorac Cardiovasc Surg* 2021. [DOI](#)
7. Bramer S, van Straten AH, Soliman Hamad MA, Berreklouw E, Martens EJ, Maessen JG. The impact of new-onset postoperative atrial fibrillation on mortality after coronary artery bypass grafting. *Ann Thorac Surg* 2010;90:443-9. [DOI](#) [PubMed](#)
8. Chebbout R, Heywood EG, Drake TM, et al. A systematic review of the incidence of and risk factors for postoperative atrial fibrillation following general surgery. *Anaesthesia* 2018;73:490-8. [DOI](#) [PubMed](#)
9. Dobrev D, Aguilar M, Heijman J, Guichard JB, Nattel S. Postoperative atrial fibrillation: mechanisms, manifestations and management. *Nat Rev Cardiol* 2019;16:417-36. [DOI](#) [PubMed](#)
10. Arsenault KA, Yusuf AM, Crystal E, et al. Interventions for preventing post-operative atrial fibrillation in patients undergoing heart surgery. *Cochrane Database Syst Rev* 2013:CD003611. [DOI](#) [PubMed](#) [PMC](#)
11. Kalman JM, Munawar M, Howes LG, et al. Atrial fibrillation after coronary artery bypass grafting is associated with sympathetic activation. *Ann Thorac Surg* 1995;60:1709-15. [DOI](#) [PubMed](#)
12. Alexandre J, Saloux E, Chequel M, et al. Preoperative plasma aldosterone and the risk of atrial fibrillation after coronary artery bypass surgery: a prospective cohort study. *J Hypertens* 2016;34:2449-57. [DOI](#) [PubMed](#)
13. Abdelhadi RH, Gurm HS, Van Wagoner DR, Chung MK. Relation of an exaggerated rise in white blood cells after coronary bypass or cardiac valve surgery to development of atrial fibrillation postoperatively. *Am J Cardiol* 2004;93:1176-8. [DOI](#) [PubMed](#)
14. Swartz MF, Fink GW, Lutz CJ, et al. Left versus right atrial difference in dominant frequency, K(+) channel transcripts, and fibrosis in patients developing atrial fibrillation after cardiac surgery. *Heart Rhythm* 2009;6:1415-22. [DOI](#) [PubMed](#) [PMC](#)
15. Garcia L, Verdejo HE, Kuzmicic J, et al. Impaired cardiac autophagy in patients developing postoperative atrial fibrillation. *J Thorac Cardiovasc Surg* 2012;143:451-9. [DOI](#) [PubMed](#)
16. Wu Q, Liu H, Liao J, et al. Colchicine prevents atrial fibrillation promotion by inhibiting IL-1 β -induced IL-6 release and atrial fibrosis in the rat sterile pericarditis model. *Biomed Pharmacother* 2020;129:110384. [DOI](#) [PubMed](#)
17. Ishii Y, Schuessler RB, Gaynor SL, Hames K, Damiano RJ. Postoperative atrial fibrillation: the role of the inflammatory response. *J Thorac Cardiovasc Surg* 2017;153:1357-65. [DOI](#) [PubMed](#) [PMC](#)
18. Robinson E, Kaushal S, Alaboson J, et al. Combinatorial release of dexamethasone and amiodarone from a nano-structured parylene-C film to reduce perioperative inflammation and atrial fibrillation. *Nanoscale* 2016;8:4267-75. [DOI](#) [PubMed](#)
19. Li N, Wehrens XH. Programmed electrical stimulation in mice. *J Vis Exp* 2010:1730. [DOI](#) [PubMed](#) [PMC](#)
20. Campbell HM, Quick AP, Abu-Taha I, et al. Loss of SPEG inhibitory phosphorylation of ryanodine receptor type-2 promotes atrial fibrillation. *Circulation* 2020;142:1159-72. [DOI](#) [PubMed](#) [PMC](#)
21. Verheule S, Sato T, Everett T, et al. Increased vulnerability to atrial fibrillation in transgenic mice with selective atrial fibrosis caused by overexpression of TGF-beta1. *Circ Res* 2004;94:1458-65. [DOI](#) [PubMed](#) [PMC](#)

22. Livak KJ, Schmittgen TD. Analysis of relative gene expression data using real-time quantitative PCR and the 2(-Delta Delta C(T)) Method. *Methods* 2001;25:402-8. [DOI](#) [PubMed](#)
23. Sadeghi N, Sadeghi S, Mood ZA, Karimi A. Determinants of operative mortality following primary coronary artery bypass surgery. *Eur J Cardiothorac Surg* 2002;21:187-92. [DOI](#) [PubMed](#)
24. Filardo G, Damiano RJ, Ailawadi G, et al. Epidemiology of new-onset atrial fibrillation following coronary artery bypass graft surgery. *Heart* 2018;104:985-92. [DOI](#)
25. Wehrens X. Mouse electrocardiography an interval of thirty years. *Cardiovasc Res* 2000;45:231-7. [DOI](#) [PubMed](#)
26. Hulsurkar MM, Lahiri SK, Moore O, et al. Atrial-Specific LKB1 knockdown represents a novel mouse model of atrial cardiomyopathy with spontaneous atrial fibrillation. *Circulation* 2021;144:909-12. [DOI](#) [PubMed](#) [PMC](#)
27. Staerk L, Wang B, Preis SR, et al. Lifetime risk of atrial fibrillation according to optimal, borderline, or elevated levels of risk factors: cohort study based on longitudinal data from the framingham heart study. *BMJ* 2018;361:k1453. [DOI](#)
28. Mariscalco G, Biancari F, Zanobini M, et al. Bedside tool for predicting the risk of postoperative atrial fibrillation after cardiac surgery: the POAF score. *J Am Heart Assoc* 2014;3:e000752. [DOI](#) [PubMed](#) [PMC](#)
29. Jansen HJ, Moghtadaei M, Rafferty SA, Rose RA. Atrial fibrillation in aging and frail mice: modulation by natriuretic peptide receptor C. *Circ Arrhythm Electrophysiol* 2021;14:e010077. [DOI](#) [PubMed](#)
30. Luo T, Chang CX, Zhou X, Gu SK, Jiang TM, Li YM. Characterization of atrial histopathological and electrophysiological changes in a mouse model of aging. *Int J Mol Med* 2013;31:138-46. [DOI](#) [PubMed](#)
31. Comelli M, Meo M, Cervantes DO, et al. Rhythm dynamics of the aging heart: an experimental study using conscious, restrained mice. *Am J Physiol Heart Circ Physiol* 2020;319:H893-905. [DOI](#) [PubMed](#) [PMC](#)
32. Zaman AG, Archbold RA, Helft G, Paul EA, Curzen NP, Mills PG. Atrial fibrillation after coronary artery bypass surgery: a model for preoperative risk stratification. *Circulation* 2000;101:1403-8. [DOI](#) [PubMed](#)
33. Chugh SS, Havmoeller R, Narayanan K, et al. Worldwide epidemiology of atrial fibrillation: a Global Burden of Disease 2010 study. *Circulation* 2014;129:837-47. [DOI](#) [PubMed](#) [PMC](#)
34. Hart RG, Pearce LA, McBride R, Rothbart RM, Asinger RW. Factors associated with ischemic stroke during aspirin therapy in atrial fibrillation: analysis of 2012 participants in the SPAF I-III clinical trials. *Stroke* 1999;30:1223-9. [DOI](#) [PubMed](#)
35. Benjamin EJ, Levy D, Vaziri SM, D'Agostino RB, Belanger AJ, Wolf PA. Independent risk factors for atrial fibrillation in a population-based cohort. *JAMA* ;271:840-844. [PubMed](#)
36. Wolf PA, Dawber TR, Thomas HE, Kannel WB. Epidemiologic assessment of chronic atrial fibrillation and risk of stroke: the Framingham study. *Neurology* 1978;28:973-7. [DOI](#) [PubMed](#)
37. Li Z, Wang Z, Yin Z, et al. Gender differences in fibrosis remodeling in patients with long-standing persistent atrial fibrillation. *Oncotarget* 2017;8:53714-29. [DOI](#) [PubMed](#) [PMC](#)
38. Ma Y, Iyer RP, Jung M, Czubryt MP, Lindsey ML. Cardiac fibroblast activation post-myocardial infarction: current knowledge gaps. *Trends Pharmacol Sci* 2017;38:448-58. [DOI](#) [PubMed](#) [PMC](#)
39. Li X, Garcia-Elias A, Benito B, Nattel S. The effects of cardiac stretch on atrial fibroblasts: analysis of the evidence and potential role in atrial fibrillation. *Cardiovasc Res* 2022;118:440-60. [DOI](#) [PubMed](#) [PMC](#)
40. Ishii Y, Schuessler RB, Gaynor SL, et al. Inflammation of atrium after cardiac surgery is associated with inhomogeneity of atrial conduction and atrial fibrillation. *Circulation* 2005;111:2881-8. [DOI](#) [PubMed](#)
41. Yao C, Veleva T, Scott L, et al. Enhanced cardiomyocyte NLRP3 inflammasome signaling promotes atrial fibrillation. *Circulation* 2018;138:2227-42. [DOI](#) [PubMed](#) [PMC](#)
42. Huang Z, Chen XJ, Qian C, et al. Signal transducer and activator of transcription 3/microRNA-21 feedback loop contributes to atrial fibrillation by promoting atrial fibrosis in a rat sterile pericarditis model. *Circ Arrhythm Electrophysiol* 2016;9:e003396. [DOI](#) [PubMed](#) [PMC](#)
43. Gaudino M, Andreotti F, Zamparelli R, et al. The -174G/C interleukin-6 polymorphism influences postoperative interleukin-6 levels and postoperative atrial fibrillation. Is atrial fibrillation an inflammatory complication? *Circulation* 2003;108:II195-9. [DOI](#) [PubMed](#)
44. Fu XX, Zhao N, Dong Q, et al. Interleukin-17A contributes to the development of post-operative atrial fibrillation by regulating inflammation and fibrosis in rats with sterile pericarditis. *Int J Mol Med* 2015;36:83-92. [DOI](#) [PubMed](#) [PMC](#)
45. Heijman J, Muna AP, Veleva T, et al. Atrial Myocyte NLRP3/CaMKII nexus forms a substrate for postoperative atrial fibrillation. *Circ Res* 2020;127:1036-55. [DOI](#) [PubMed](#) [PMC](#)
46. Tsai FC, Lin YC, Chang SH, et al. Differential left-to-right atria gene expression ratio in human sinus rhythm and atrial fibrillation: implications for arrhythmogenesis and thrombogenesis. *Int J Cardiol* 2016;222:104-12. [DOI](#) [PubMed](#)
47. Kahr PC, Piccini I, Fabritz L, et al. Systematic analysis of gene expression differences between left and right atria in different mouse strains and in human atrial tissue. *PLoS One* 2011;6:e26389. [DOI](#) [PubMed](#) [PMC](#)
48. Goya S, Wada T, Shimada K, Hirao D, Tanaka R. Dose-dependent effects of isoflurane and dobutamine on cardiovascular function in dogs with experimental mitral regurgitation. *Vet Anaesth Analg* 2018;45:432-42. [DOI](#) [PubMed](#)
49. Shintaku T, Ohba T, Niwa H, et al. Effects of isoflurane inhalation anesthesia on mouse ECG. *Hirosaki Med J* 2015;66:1-7. [DOI](#)